Scattering experiments with a diving cylinder

Michael Paulus[1,2] **and Olivier J. F. Martin**[1]

[1] *Electromagnetic Fields and Microwave Electronics Laboratory*
Swiss Federal Institute of Technology, ETH–Zentrum, ETZ
CH-8092 Zurich, Switzerland

[2] *IBM Research, Zurich Research Laboratory*
CH-8803 Rüschlikon, Switzerland

paulus@ifh.ee.ethz.ch,martin@ifh.ee.ethz.ch
http://www.ifh.ee.ethz.ch/~martin

Abstract: We present numerical experiments of light scattering by a circular dielectric cylinder embedded in a stratified background, using the Green's tensor technique. The stratified background consists of two or three dielectric layers, the latter forming an anti–reflection system. We show movies of the scattered field as a function of different parameters: polarization, angle of incidence, and relative position of the cylinder with respect to the background interfaces.

OCIS codes: (240.0240) Optics at surfaces; (260.3160) Interference; (260.5430) Polarization; (290.0290) Scattering; (310.1620) Coatings.

References and links

1. Lord Rayleigh, "On the Electromagnetic Theory of Light," Philos. Mag. **12,** 81–101 (1881).
2. T. C. Rao and R. Barakat, "Plane–wave scattering by a conducting cylinder partially buried in a ground plane. 1. TM case," J. Opt. Soc. Am. A **6,** 1270–1280 (1989).
3. T. C. Rao and R. Barakat, "Plane–wave scattering by a conducting cylinder partially buried in a ground plane II: TE case," J. Opt. Soc. Am. A **8,** 1986–1990 (1991).
4. G. Videen and D. Ngo, "Light scattering from a cylinder near a plane interface: theory and comparison with experimental data," J. Opt. Soc. Am. A **14,** 70–78 (1997).
5. P. J. Valle, F. González, and F. Moreno, "Electromagnetic wave scattering from conducting cylindrical structures on flat substraes: study by means of the extinction theorem," Appl. Opt. **33,** 512–523 (1994).
6. A. Madrazo and M. Nieto-Vesperinas, "Scattering of electromagnetic waves from a cylinder in front of a conducting plane," J. Opt. Soc. Am. A **12,** 1298–1309 (1995).
7. R. Borghi, F. Gori, M. Santarsiero, F. Frezza, and G. Schettini, "Plane–wave scattering by a perfectly conducting circular cylinder near a plane surface: cylindrical–wave approach," J. Opt. Soc. Am. A **13,** 483–493 (1996).
8. R. Borghi, M. Santarsiero, F. Frezza, and G. Schettini, "Plane–wave scattering by a dielectric circular cylinder parallel to a general reflecting flat surface," J. Opt. Soc. Am. A **14,** 1500–1504 (1997).
9. J.–J. Greffet, "Scattering of s–polarized electromagnetic waves by a 2d obstacle near an interface," Opt. Commun. **72,** 274–278 (1989).
10. M. A. Taubenblatt, "Light scattering from cylindrical structures on surfaces," Opt. Lett. **15,** 255–257 (1990).
11. F. Pincemin, A. Sentenac, and J.–J. Greffet, "Near field scattered by a dielectric rod below a metallic surface," J. Opt. Soc. Am. A **11,** 1117–1127 (1994).
12. N. P. Zhuck and A. G. Yarovoy, "Two–Dimensional Scattering from an Inhomogeneous Dielectric Cylinder Embedded in a Stratified Medium: Case of TM Polarization," IEEE Trans. Antennas & Propag. **42,** 16–21 (1994).
13. M. Totzeck and H. J. Tiziani, "Interference microscopy of sub–λ structures: A rigorous computation method and measurements," Opt. Commun. **136,** 61–74 (1997).

#34836 - $15.00 US
Received July 20, 2001; Revised September 05, 2001

14. M. Paulus and O. J. F. Martin, "Green's tensor technique for scattering in 2D stratified media," Phys. Rev. E **63,** 066615.1–066615.8 (2001).
15. O. J. F. Martin and N. B. Piller, "Electromagnetic scattering in polarizable backgrounds," Phys. Rev. E **58,** 3909–3915 (1998).
16. J. D. Jackson, *Classical electrodynamics*, 3rd ed. (Wiley, New York, 1999).
17. O. J. F. Martin, C. Girard, and A. Dereux, "Dielectric vs. topographic contrast in near–field microscopy," J. Opt. Soc. Am. A **13,** 1801–1808 (1996).
18. C. F. Bohren and D. R. Huffman, *Absorption and scattering of light by small particles* (Wiley, New York, 1983).
19. M. Born and E. Wolf, *Principles of Optics*, 6th. ed. (Pergamon Press, Oxford, 1987).

1 Introduction

The optical properties of cylindrical particles have generated a lot of interest, as they provide a simple model for specific physical systems. The scattering on a cylinder situated in an infinite homogeneous background was for example already treated by Lord Rayleigh in 1881 [1].

However, most real situations are more complex, the particles are located on a substrate or embedded in an even more complicated stratified background. To investigate such geometries many analytical and numerical approaches were developed. They include, for example, image methods [2–4], applications of the extinction theorem [5, 6], expansions of cylindrical waves [7, 8] or integral–equation methods [9–13]. Most of these methods only consider a background medium consisting of two half spaces [2–11] or restrict the choice of the material or geometry parameters [2–5, 7].

Recently, we presented a general technique for light propagation and scattering in two–dimensional (2D) structures formed by a stratified background with embedded scatterers [14]. This approach is based on the Green's tensor associated with the stratified background and provides a rigorous solution of the vectorial wave equation with the boundary conditions given at the different material interfaces.

In this paper we apply our approach to study the light scattered by a dielectric circular cylinder in the presence of a stratified dielectric background. We investigate the different phenomena that can occur, depending on the relative cylinder position with respect to the background interfaces, as well as on the illumination direction.

In Sec. 2 we briefly recall our computational approach and in Sec. 3 we show calculations of the total electric field amplitude $A = \sqrt{\mathbf{E} \cdot \mathbf{E}^*}$ as a function of different geometrical and illumination parameters. Our results are summarized in Sec. 4.

2 Model

Throughout the paper we consider a circular cylinder with radius $r = 150\,\mathrm{nm}$ and permittivity $\varepsilon_{\mathrm{Cyl}} = 2$ embedded in a two– or three–layer background. This system is illuminated from the top with a plane wave under different angles of incidence Θ. The illumination wavelength is $\lambda = 633\,\mathrm{nm}$ and two different polarizations are considered: s polarization, with the electric field $\mathbf{E}^0$ in y direction, and p polarization with the electric field $\mathbf{E}^0$ lying in the xz plane.

Since the scattering geometry under study is translation invariant in y direction we can restrict the investigation to a cross section in the xz plane [14]. When such a system formed by a stratified background (L layers, permittivity ε_l, $l = 1, \ldots, L$) with embedded scatterers is illuminated with an incident field $\mathbf{E}^0(\mathbf{r})$ propagating in the stratified background [we consider harmonic fields with time dependence $\exp(-i\omega t)$], the total field $\mathbf{E}(\mathbf{r})$ is given by the electric field integral equation:

$$\mathbf{E}(\mathbf{r}) = \mathbf{E}^0(\mathbf{r}) + \int_{\mathrm{A}} \mathrm{d}\mathbf{r}' \mathbf{G}(\mathbf{r}, \mathbf{r}') \cdot k_0^2 \Delta\varepsilon(\mathbf{r}') \mathbf{E}(\mathbf{r}')\,, \tag{1}$$

#34836 - $15.00 US Received July 20, 2001; Revised September 05, 2001

where $\mathbf{G}(\mathbf{r},\mathbf{r}')$ is the Green's tensor associated with the stratified background, $k_0^2 = \omega^2\varepsilon_0\mu_0$ the vacuum wave number and $\Delta\varepsilon(\mathbf{r})$ the dielectric contrast:

$$\Delta\varepsilon(\mathbf{r}) = \varepsilon(\mathbf{r}) - \varepsilon_\kappa\,, \quad \mathbf{r} \in \text{layer } \kappa\,. \tag{2}$$

Whereas the Green's tensor for an infinite homogeneous background can be expressed analytically [15], this is not possible when the background is stratified. In this case $\mathbf{G}(\mathbf{r},\mathbf{r}')$ must be computed numerically with Sommerfeld type integrals [14].

Since the integration in Eq. (1) runs only over the scatterer section A, the discretization is limited to this volume, the stratified background being accounted for by the Green's tensor. Another advantage of this method is that the boundary conditions at the different material interfaces, as well as at the edges of the computation window are perfectly and automatically fulfilled [14, 15].

3 Results

3.1 *Homogeneous space*

Before studying complex effects that can arise when the cylinder is placed in a stratified background, it is educational to review the simpler case of the scattering by a cylinder in an infinite homogeneous space $\varepsilon_\mathrm{H} = 1$. Figure 1 shows the total electric field amplitude in such a system for both s and p polarizations, when the cylinder is illuminated with an incident electric field $\mathbf{E}^0$ propagating in $-z$ direction:

$$\mathbf{E}^0(x,z) = \mathbf{A}^0 \exp(i\mathbf{kr}) = \mathbf{A}^0 \exp(ik_z z)\,, \tag{3}$$

where $\mathbf{A}^0$ is the amplitude vector with $|\mathbf{A}^0| = 1$, $\mathbf{k} = (k_x, k_z)$ is the wave vector of the incident wave and $k_z = -|\mathbf{k}|$. (For all the calculations we normalize the electric field amplitude of the incident field $|\mathbf{A}^0| = (\mathbf{E}^0 \cdot \mathbf{E}^{0*})^{1/2} = 1$.)

Some features of the field distributions in Fig. 1 are common to both polarizations: in backward direction stationary waves are created due to the interference of the incident and the reflected waves. In the forward direction we recognize the diffraction pattern of the cylinder. However, the near field distribution at close vicinity of the cylinder strongly depends on the polarization of the incident field. For s polarization a maximum of the intensity can be observed inside the cylinder whereas for p polarization two peaks occur on the left and right sides of the scatterer. This behavior can be explained with the

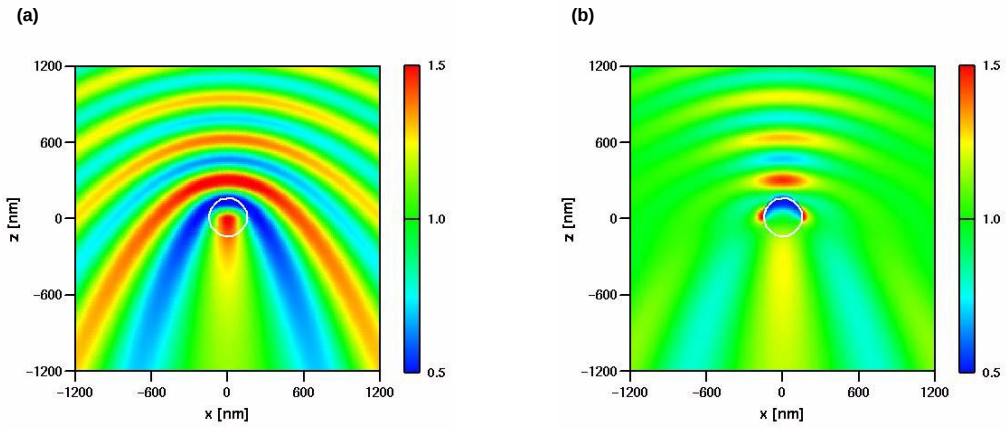

Fig. 1. Electric field amplitude distribution for the scattering by a cylinder in an infinite homogeneous background. Two different polarizations are investigated: (a) s polarization, (b) p polarization.

#34836 - $15.00 US Received July 20, 2001; Revised September 05, 2001

boundary conditions resulting from Maxwell's equations. When the electric field $\mathbf{E}$ is parallel to a material interface it must be continuous [16]. When it is normal to the interface, it is the displacement field $\mathbf{D} = \varepsilon\mathbf{E}$ which must be continuous. Hence, for a p–polarized excitation the total electric field amplitude is discontinuous by a factor $\varepsilon_{\mathrm{Cyl}}/\varepsilon_{\mathrm{H}}$ wherever the incident field is normal to a material interface (i.e. on the left and right sides of the cylinder in Fig. 1(b)). Such depolarization effects do not occur at the top and bottom sides of the cylinder for p polarization [Fig. 1(b)] or on the entire circumference for s polarization [Fig. 1(a)], since in those locations the incident field is parallel to the material interfaces [17].

As a consequence of the depolarization effects for a p–polarized excitation, the forward scattered light is focussed by the cylinder and reaches a maximum at $z \approx -300\,\mathrm{nm}$. For s polarization, on the other hand, the field maximum is situated inside the cylinder.

The total scattering cross section of a dielectric circular cylinder is greater for s polarization than for p polarization, the difference increasing with a larger dielectric contast [18]. As a matter of fact, we observe in Fig. 1(a) a more pronounced interference pattern than in Fig. 1(b). This polarization dependence of the total scattering cross section is also observable for all further configurations under study.

3.2 *Scattering in the presence of a surface*

Now we divide the background into two half spaces $\varepsilon_1 = 1$ $(z \geq 0)$ and $\varepsilon_2 = 2$ $(z < 0)$, in such a way that the lower layer has the same permittivity as the cylindrical scatterer, $\varepsilon_2 = \varepsilon_{\mathrm{Cyl}}$.

The movies in Fig. 2 show the response of the system under normal incidence $(\Theta = 0)$ for s– and p–polarized illumination. Each movie frame corresponds to a given distance h between the cylinder center and the material interface.

Since the incident wave is now reflected back at the plane interface, the illumination electric field becomes in the top layer

$$\mathbf{E}^0(x,z) = \mathbf{A}^0[\exp(ik_{1z}z) + R\exp(-ik_{1z}z)]\,, \quad z \geq 0\,, \tag{4}$$

and in the bottom layer

$$\mathbf{E}^0(x,z) = \mathbf{A}^0\,T\exp(ik_{2z}z)\,, \quad z < 0\,, \tag{5}$$

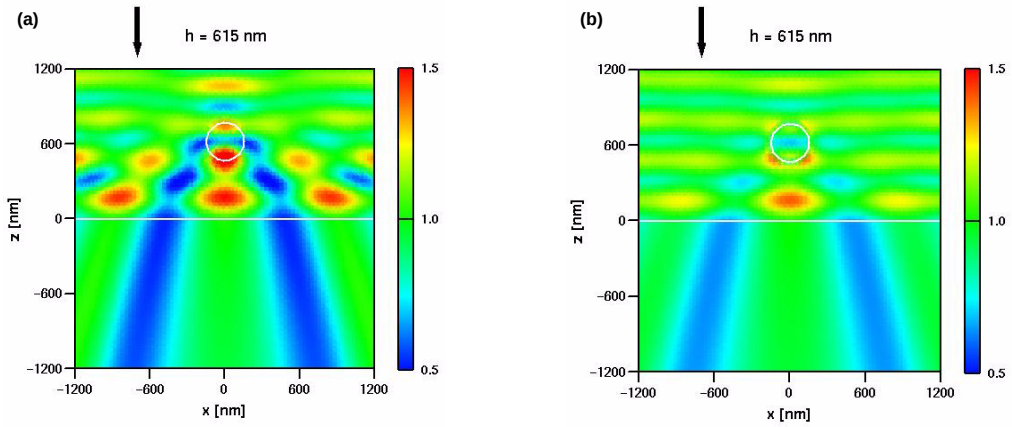

Fig. 2. Electric field amplitude distribution for the scattering by a cylinder above a dielectric surface with same permittivity, as a function of the distance h between the cylinder center and the interface. Normal incidence ($\Theta = 0^{\mathrm{o}}$, the arrow represents the propagation direction of the illumination wave) (a) s polarization (528 KB), (b) p polarization (479 KB).

#34836 - $15.00 US Received July 20, 2001; Revised September 05, 2001

where k_{iz}, $i = 1, 2$, is the z component of the wave vector in layer i, R is the Fresnel reflection coefficient and T the corresponding transmission coefficient for normal incidence [19]:

$$R = \frac{\sqrt{\varepsilon_1} - \sqrt{\varepsilon_2}}{\sqrt{\varepsilon_1} + \sqrt{\varepsilon_2}}\,, \tag{6}$$

$$T = \frac{2\sqrt{\varepsilon_1}}{\sqrt{\varepsilon_1} + \sqrt{\varepsilon_2}}\,. \tag{7}$$

Note that R and T are real for absorptionless media. The negative reflection coefficient obtained in our system leads to a phase shift of 180° for the reflected field.

The illumination amplitude in the upper half space reads now

$$A = (\mathbf{E}^0 \cdot \mathbf{E}^{0*})^{\frac{1}{2}} = |\mathbf{A}^0|\,[1 + R^2 + 2R\cos(2k_{1z}z)]^{\frac{1}{2}}\,, \quad z \geq 0\,, \tag{8}$$

and a stationary wave with period $\Delta = \pi/k_{1z} = \lambda/2$ is created in the upper half space (Fig. 2). Because of $R < 0$ the amplitude is minimal directly at the interface.

The cylinder is not anymore illuminated by a homogeneous plane wave but moves in the field of the stationary wave. Hence, in the top layer the total field distribution is a superposition of the stationary wave and a diffraction pattern similar to that in Fig. 1. This pattern determines also the field distribution in the bottom layer depending on the transmittance of the interface.

As in the case of the homogeneous background the near field of the cylinder depends on the polarization of the excitation. Additionally, the location and strength of the scattered field maxima are modulated by the cylinder altitude h.

The stationary wave itself is further amplified in the region between the cylinder and the interface. This is caused both by the focusing provided by the cylinder and by multiple reflections between the surface and the cylinder. Note also that the interaction between the excitation and the field scattered by the cylinder creates an interference pattern in x direction.

For $h = -15$ nm, when half of the cylinder is included in the surface, most of the backscattering disappears in a narrow sector of the upper halfspace. Finally, for $h = -165$ nm the cylinder is entirely immersed in the lower layer with identical permittivity, and the total electric field is simply given by the excitation in the stratified background. Since without the cylinder s and p polarization are indistinguishable for normal incidence, the field distributions are identical in both frames.

Let us now rotate the angle of incidence Θ with respect to the surface normal. Figure 3 shows again the scattering as a function of the cylinder altitude h, but for $\Theta = 30^{\circ}$.

In this case, the illuminating electric field in the top layer becomes

$$E^0_\alpha(x, z) = A^0_\alpha[\exp(ik_{1z}z) + R_\alpha \exp(-ik_{1z}z)]\exp(ik_x x)\,, \quad z \geq 0\,, \quad \alpha = x, y, z\,, \tag{9}$$

where the reflection coefficients correspond to the polarization of the given component: $R_x = -R^{\mathrm{p}}$, $R_y = R^{\mathrm{s}}$, and $R_z = R^{\mathrm{p}}$. In this case of non–normal illumination, the Fresnel coefficients $R^{\mathrm{s/p}}$ depend on the polarization of the incident wave [19]:

$$R^{\mathrm{s}} = \frac{k_{1z} - k_{2z}}{k_{1z} + k_{2z}}\,, \tag{10}$$

$$R^{\mathrm{p}} = \frac{\varepsilon_2 k_{1z} - \varepsilon_1 k_{2z}}{\varepsilon_2 k_{1z} + \varepsilon_1 k_{2z}}\,. \tag{11}$$

The illumination amplitude in the upper half space is then

$$\begin{aligned} A \;=\; & \{{A^0_x}^2[1 + {R^{\mathrm{p}}}^2 - 2R^{\mathrm{p}}\cos(2k_{1z}z)] + {A^0_y}^2[1 + {R^{\mathrm{s}}}^2 + 2R^{\mathrm{s}}\cos(2k_{1z}z)] \\ & + {A^0_z}^2[1 + {R^{\mathrm{p}}}^2 + 2R^{\mathrm{p}}\cos(2k_{1z}z)]\}^{\frac{1}{2}}\,, \quad z \geq 0\,. \end{aligned} \tag{12}$$

#34836 - $15.00 US Received July 20, 2001; Revised September 05, 2001

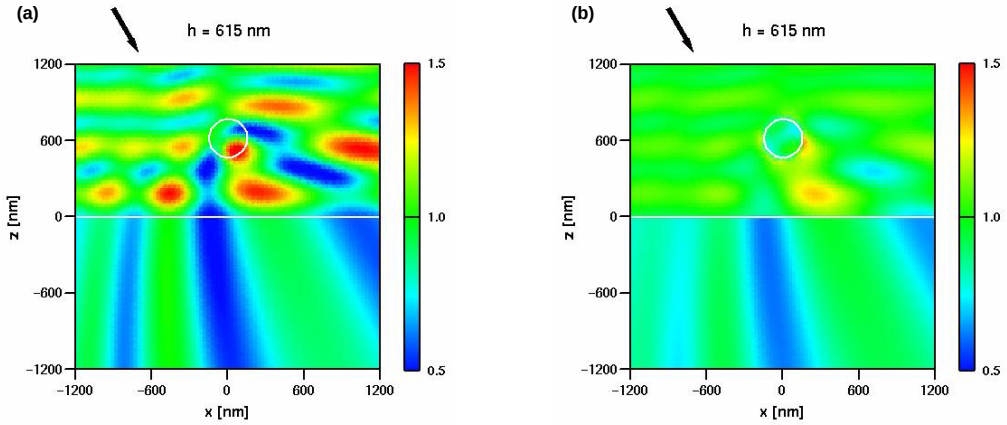

Fig. 3. Same situation as in Fig. 2, but now the illumination field is incident at a $\Theta = 30^{\circ}$ angle. (a) s polarization (530 KB), (b) p polarization (452 KB).

Again, a stationary wave excites the cylinder, but the period is now increased to $\Delta = \pi/k_z = \lambda/(2\cos\Theta) = \lambda/\sqrt{3}$.

The diffraction patterns and position of the near field maxima rotate accordingly to the change of the incidence angle (compare Figs. 2 and 3). For p polarization, one of the two field maxima previously visible on the lateral sides of the cylinder (Fig. 1) disappears and only a maximum is now visible on the right, in the direction of the illumination momentum (Fig. 3).

The computer experiments reported in Fig. 3 also illustrate the polarization dependence of the boundary conditions at the interface between the two layers: for s polarization the electric field must be continuous, whereas p polarization enforces a discontinuity proportional to the ratio $\varepsilon_1/\varepsilon_2$.

To further investigate the effect of the angle of incidence Θ, we show in Fig. 4 movies for a fixed cylinder altitude $h = 615\,\mathrm{nm}$ and a varying illumination angle Θ.

As expected, the period of the stationary wave increases for larger angles Θ and the diffraction pattern becomes more and more twisted (Fig. 4). Since the reflection coefficients $R^{\mathrm{s/p}}$ of the interface approach 1 in the limit $\Theta = 90^{\circ}$, the field transmitted

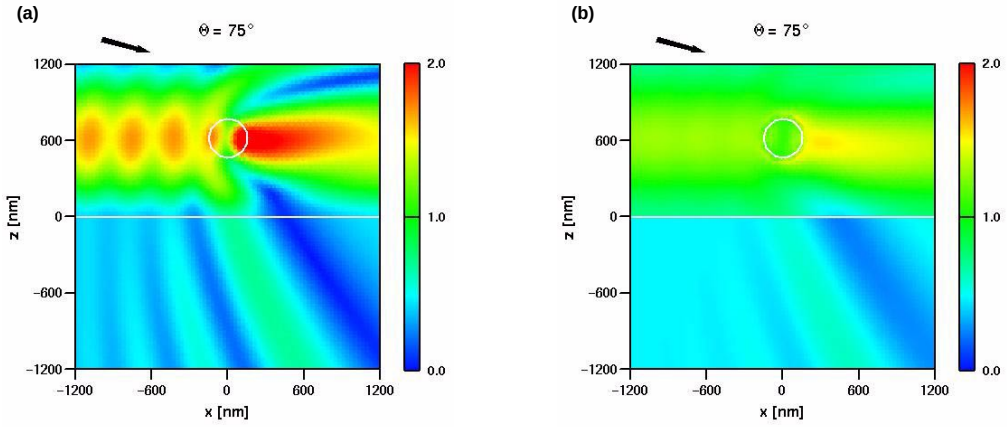

Fig. 4. Electric field amplitude distribution for the scattering by a cylinder above a dielectric surface with same permittivity, as a function of the illumination angle Θ (the arrow indicates the propagation direction of the illumination field). The cylinder position is kept fixed: $h = 615\,\mathrm{nm}$. (a) s polarization (227 KB), (b) p polarization (204 KB).

#34836 - $15.00 US
Received July 20, 2001; Revised September 05, 2001

into the lower half space vanishes for larger angles and the amplitude maxima of the stationary wave converge towards their upper value for total reflection $A = 2$ (see Eq. (12) with $k_z \to 0$ and $R^{\mathrm{s/p}} \to 1$). This produces a strong scattering both in forward and in backward direction when the maximum of the stationary wave coincides with the cylinder altitude ($\Theta = 75^{\mathrm{o}}$, Fig. 4).

At first sight, it may be surprising that in the case of p polarization the stationary wave in the top layer vanishes for $\Theta \approx 40^{\mathrm{o}}$–$60^{\mathrm{o}}$, and only the field scattered by the cylinder can be observed [Fig. 4(b)]. Depending on the angle, two different mechanisms contribute to this behavior. First, for $\Theta = 45^{\mathrm{o}}$ the x and z components of the p–polarized illumination electric field are identical, $A_x^0 = A_z^0$, and Eq. (12) becomes

$$A = |\mathbf{A}^0| \, (1 + R^{\mathrm{p}2})^{\frac{1}{2}} \, . \tag{13}$$

Hence, the z dependence of $\mathbf{E} \cdot \mathbf{E}^*$ is cancelled out.

To illustrate the second mechanism we report in Fig. 5 the amplitude A_{refl} reflected by a plane interface between two half spaces $\varepsilon_1 = 1$ and $\varepsilon_2 = 2$, as a function of the angle of incidence Θ. At $\Theta \approx 55^{\mathrm{o}}$, the Brewster angle of the material system under study, $A_{\mathrm{refl}} = 0$. At this angle, the reflectivity vanishes for p–polarized plane waves and all the energy of the incident field is transmitted into the lower half space. Note however that zero reflectivity does *not* imply that the amplitude of the transmitted light T in the bottom layer is 1 [19]. A straightforward calculation gives $T = \sqrt{\varepsilon_1/\varepsilon_2}$, which yields in our case $T \approx 0.75$, in perfect agreement with our calculations. Both above–mentioned phenomena do not exist for s polarization.

In Fig. 5 we can further observe that on the entire angle range s polarization leads to a larger reflectivity. This behavior is similar to the polarization dependence of the scattering on a cylinder (see Sec. 3.1).

3.3 *Anti–reflection layer*

In the following, we add a third layer to create a structure with $\varepsilon_1 = 1$, $\varepsilon_2 = 1.334$, and $\varepsilon_3 = 1.78$. This structure represents an air/water system, separated by an intermediated slab acting as anti–reflection layer [19]. For normal incidence on the material interfaces, the reflectivity is indeed strictly zero only if the permittivities are connected by

$$\varepsilon_2 = \sqrt{\varepsilon_1 \varepsilon_3} \approx 1.334 \, , \tag{14}$$

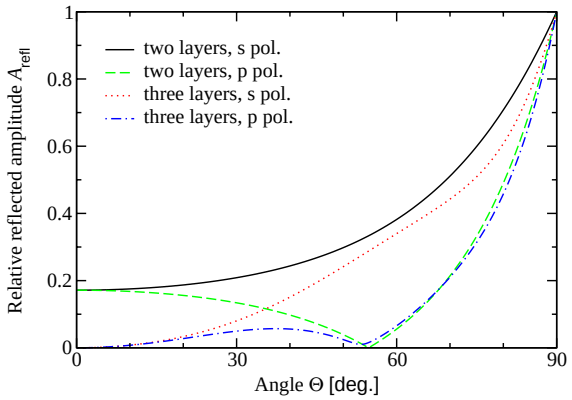

Fig. 5. Relative reflected amplitude A_{refl} for a two–layer medium with $\varepsilon_1 = 1$, $\varepsilon_2 = 2$, and a three–layer medium with $\varepsilon_1 = 1$, $\varepsilon_2 = 1.334$, $\varepsilon_3 = 1.78$, as a function of the angle of incidence Θ. Incident s and p polarizations are compared. The minima for p polarization correspond to the Brewster angle.

#34836 - $15.00 US
Received July 20, 2001; Revised September 05, 2001

and the thickness d of the slab is

$$d = \left(n + \frac{1}{2}\right) \frac{\lambda}{2\sqrt{\varepsilon_2}}, \quad n = 1, 2, 3, ... \tag{15}$$

Taking $n = 2$ in Eq. (15), we use for our calculations $d = 411\,\text{nm}$, so that the cylinder fits within the antireflection layer.

The movies in Fig. 6 clearly illustrate that, independent of the cylinder location, there is no stationary wave in the top layer due to reflection of the illuminating field by the slab. Striking in these movies is the fact that the antireflection layer remains very efficient, even in the presence of the cylinder. Again, it is the s–polarized illumination which produces a weak interference pattern. To explain this behavior, in Fig. 5 we also report the reflected amplitude A_{refl} for the three–layer system under study. Similar to the case of the single interface, s polarization leads to a stronger scattering for all angles Θ and, consequently, to an enhanced backreflection of the field components scattered by the cylinder and impinging at non–normal incidence on the interface. Note also that $A_{\text{refl}} = 0$ for $\Theta = 0^{\text{o}}$ since we designed the slab to be reflectionless. Further, in Fig. 5 we observe that for p polarization the Brewster angle is slightly shifted to $\Theta \approx 53^{\text{o}}$, and the corresponding reflected amplitude does not vanish completely for that three-layers system.

4 Summary

When a cylindrical particle is located in a stratified background, the resulting electric field distribution is determined by the interaction between the cylinder and the different material interfaces. In this paper, we used the Green's tensor technique to illustrate the scattering phenomena occurring in such structures. The Green's tensor technique is very well adapted to this kind of geometry because the optical processes in the layered material system are accurately described by the Green's tensor. Further, only the cylinder needs to be discretized, irrespective of the number of layers forming the stratified background. Our calculations illustrate the complexity of the phenomena that can occur in such a rather simple system, depending on the relative position of the cylinder to the different material interfaces.

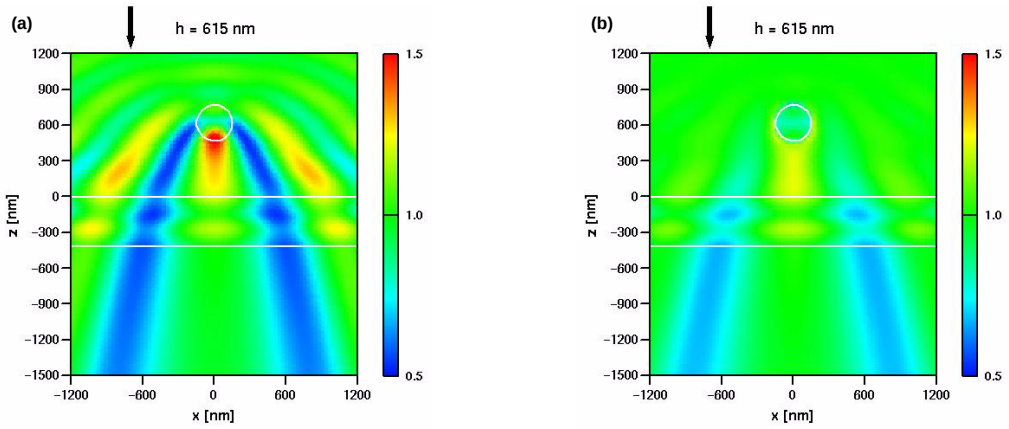

Fig. 6. Electric field amplitude distribution for the scattering by a cylinder in a three–layer system, including an anti–reflection slab, as a function of the cylinder altitude h above the top interface. Normal incidence ($\Theta = 0^{\text{o}}$, the arrow represents the propagation direction of the illumination wave). (a) s polarization (1052 KB), (b) p polarization (959 KB).

#34836 - $15.00 US
Received July 20, 2001; Revised September 05, 2001

Acknowledgments

It is a pleasure to thank B. Michel (IBM) for his support of the project. We gratefully acknowledge funding from the Swiss National Science Foundation.

#34836 - $15.00 US Received July 20, 2001; Revised September 05, 2001